



LAWRENCE
LIVERMORE
NATIONAL
LABORATORY

Anodic Behavior of Specimens Prepared from a Full-Diameter Alloy 22 Fabricated Container

Kenneth J. King, John C. Estill, Raúl B. Rebak

February 10, 2005

ASME Pressure Vessels & Piping Division Conference
Denver, CO, United States
July 17, 2005 through July 21, 2005

Disclaimer

This document was prepared as an account of work sponsored by an agency of the United States Government. Neither the United States Government nor the University of California nor any of their employees, makes any warranty, express or implied, or assumes any legal liability or responsibility for the accuracy, completeness, or usefulness of any information, apparatus, product, or process disclosed, or represents that its use would not infringe privately owned rights. Reference herein to any specific commercial product, process, or service by trade name, trademark, manufacturer, or otherwise, does not necessarily constitute or imply its endorsement, recommendation, or favoring by the United States Government or the University of California. The views and opinions of authors expressed herein do not necessarily state or reflect those of the United States Government or the University of California, and shall not be used for advertising or product endorsement purposes.

ANODIC BEHAVIOR OF SPECIMENS PREPARED FROM A FULL-DIAMETER ALLOY 22 FABRICATED CONTAINER

Kenneth J. King

John C. Estill

Raúl B. Rebak

Lawrence Livermore National Laboratory
7000 East Ave, L-631
Livermore, California, 94550 USA

ABSTRACT

Alloy 22 (N06022) has been extensively tested for general and localized corrosion behavior both in the wrought and annealed condition and in the as-welded condition. The specimens for testing were mostly prepared from flat plates of material. It was important to determine if the process of fabricating a full diameter Alloy 22 container will affect the corrosion performance of the alloy. Specimens were prepared directly from a fabricated container and tested for corrosion resistance. Results show that both the anodic corrosion behavior and the localized corrosion resistance of specimens prepared from a welded fabricated container was the same as from flat welded plates.

Keywords: N06022, Container Fabrication, Welding, Corrosion Rate, Repassivation Potential

INTRODUCTION

Alloy 22 (N06022) was selected by expert elicitation as the material for the corrosion resistant outer barrier.¹ Alloy 22 belongs to the family of the Nickel (Ni)-Chromium (Cr)-Molybdenum (Mo) corrosion resistant alloys.²⁻³ Alloy 22 has been extensively characterized in the laboratory for its

resistance to general or passive corrosion, localized corrosion and stress corrosion cracking.¹

A full-diameter, quarter-length mockup of the Alloy 22 was package has been fabricated for testing (Figure 21 in Reference 1).¹ It was important to test the corrosion resistance of specimens prepared from the full-diameter fabricated container to determine if industrial processes such as cold rolling, welding and annealing may affect the corrosion behavior of Alloy 22.

EXPERIMENTAL

Preparation of the Specimens

Alloy 22 (N06022) specimens were machined from 2-inch diameter hockey-puck shaped samples, which were cut from the full diameter container prototype.¹ The heat number of the base plate used for fabrication was 058371LE2 and the heat number for the weld wire was XX1829BG. The chemical composition of these two materials is not currently available. The weld seam in the hockey pucks was approximately 1-3/16" wide. The hockey pucks used to fabricate the specimens were designated: L2, L3, L4, L5, L6 and L7. That is, from six hockey pucks twelve specimens were fabricated. The prism

crevice assembly (PCA) specimens were fabricated at LTI (Hatfield, PA) and labeled from AY001 to AY012. The tested surface area of the PCA specimens was 14.06 cm². The crevicing mechanism for these PCA tests was based on ASTM G 48 12-tooth washer.⁴⁻⁶ To provide a tight crevice, the washer was made of a ceramic material and it was covered by PTFE tape. The PCA specimens were degreased in acetone and DI water, let dry before testing.

Electrolyte Solutions and Testing Procedures

Electrochemical tests were carried in deaerated simple salt solutions listed in Table 1. Nitrogen (N₂) was purged through the solution at a flow rate of 100 cc/min for 24 hours while the corrosion potential (E_{corr}) was monitored. Nitrogen bubbling was carried throughout all the electrochemical tests. The electrochemical tests were conducted in a one-liter, three-electrode, borosilicate glass flask (ASTM G 5).⁷ A water-cooled condenser combined with a water trap was used to maintain solution concentration and controlled atmosphere. The temperature of the solution was controlled using a heating mantle and a thermocouple immersed in the solution. All the tests were carried at ambient pressure. The reference electrode was saturated silver chloride (SSC) electrode, which has a potential of 199 mV more positive than the standard hydrogen electrode (SHE). The reference electrode was connected to the solution through a water-jacketed Luggin probe so that the electrode was maintained at near ambient temperature. The counter electrode was a flag (36 cm²) of platinum foil spot-welded to a platinum wire. All the potentials in this paper are reported in the SSC scale.

Basically the test sequence for each specimen consisted of three parts: (1) E_{corr} evolution as a function of time for 24 h, (2) Polarization Resistance (ASTM G 59) three subsequent times and (3) A larger anodic polarization to determine susceptibility to crevice corrosion. The larger anodic polarization was conducted using Cyclic Potentiodynamic Polarization (CPP) method (ASTM G 61).⁷

Polarization Resistance (ASTM G 59): Corrosion rates (CR) were obtained using the polarization resistance method (ASTM G 59).⁷ Each one of these tests lasts approximately four minutes. An initial potential of 20 mV below the corrosion potential (E_{corr}) was ramped to a final potential of 20 mV above E_{corr} at a rate of 0.167 mV/s. Linear fits were constrained to the potential range of 10 mV below E_{corr} to 10 mV above E_{corr} putting the potential in the X-axis. The Tafel constants, b_a and b_c, were assumed to be + 0.12 V/decade. Corrosion rates were calculated using Equation 1

$$i_{corr} = \frac{1}{R_p} \times \frac{b_a \cdot b_c}{2.303(b_a + b_c)} \quad \text{and}$$

$$CR(\mu\text{m} / \text{yr}) = k \frac{i_{corr}}{d} EW \quad (1)$$

Where k is a conversion factor (3.27 x 10⁹ nm·g·A⁻¹·cm⁻¹·yr⁻¹), i_{corr} is the measured corrosion current density in A/cm², EW is the equivalent weight, and d is the density of Alloy 22 (8.69 g/cm³). Assuming an equivalent dissolution of the major alloying elements as Ni²⁺, Cr³⁺, Mo⁶⁺, Fe²⁺, and W⁶⁺, the EW for Alloy 22 is 23.28 (ASTM G 102).⁷

Cyclic Potentiodynamic Polarization - CPP (ASTM G 61): The test to assess the susceptibility of Alloy 22 to localized corrosion and passive stability was the cyclic potentiodynamic polarization technique, CPP (ASTM G 61).⁷ The potential scan was started 100 mV below E_{corr} at a set scan rate of 0.167 mV/s. The scan direction was reversed when the current density reached 5 mA/cm² in the forward scan. Depending on the range of applied potentials, each CPP test could last between 1 h and 3 h. From the polarization curve, several parameters of importance can be extracted. The E20 and E200 represent values of breakdown potential in the forward scan of the CPP and ER10, ER1 represent values of repassivation potential in the reverse scan of the CPP. ERCO is the potential at which the reverse scan intersects the forward scan and it is also a repassivation potential.⁴⁻⁵ Table 2 lists these parameters for all the tested specimens.

RESULTS AND DISCUSSION

The Corrosion Potential (24-h)

Table 2 shows the average 24-h E_{corr} of the Alloy 22 specimens prepared using hockey pucks removed from the mockup container for six different deaerated electrolyte solutions. The values in Table 2 are short term E_{corr} in deaerated solutions and may not represent the steady-state E_{corr} for the alloy exposed to the same electrolytes for long time in aerated conditions. The 24-h E_{corr} values were surprisingly reproducible, except for the 6 m NaCl + 0.9 m KNO₃ ([Cl⁻]/[NO₃⁻]= 6.67) at 80°C. The lowest E_{corr} corresponded to the 1 M NaCl at 90°C and the highest E_{corr} corresponded to the most concentrated solution, which is also the solution with the highest concentration of nitrate (12 m CaCl₂ + 6 m Ca(NO₃)₂ [Cl⁻]/[NO₃⁻]= 6.67 at 130°C). The 24-h E_{corr} did not depend on the chloride over nitrate ratio, even though the comparison is not direct since the temperatures were different. The E_{corr} in 6 m NaCl + 0.9 m KNO₃ ([Cl⁻]/[NO₃⁻]= 6.67) seemed to –as expected- decrease when the temperature increased from 80°C to 100°C.

The Corrosion Rate (After 24-h Immersion)

Table 2 shows the average corrosion rates for the Alloy 22 specimens prepared from the hockey pucks that were removed from the mockup container. These corrosion rates were obtained after 24 h exposure in deaerated electrolytes. It is expected that the corrosion rate will decrease for longer immersion times.⁸ In spite of the short exposure time, the corrosion rates in Table 2 were low (less than 1 $\mu\text{m}/\text{year}$). The highest measured corrosion rate corresponded to the 1 M NaCl solution at 90°C (which had the lowest or more active E_{corr}) and the lowest corrosion rate was for the 12 m $\text{CaCl}_2 + 6 \text{ m Ca}(\text{NO}_3)_2$ solution even though this electrolyte had the highest temperature (130°C) (but appropriately had also the highest E_{corr}). The corrosion rate for the Alloy 22 specimens in the other four solutions (Table 2) were similar and between 0.2 and 0.4 $\mu\text{m}/\text{year}$.

Cyclic Potentiodynamic Polarization (CPP)

Table 2 shows parameters obtained from the cyclic potentiodynamic polarization (CPP) curves from the 12 tested specimens. These parameters can be divided between breakdown potentials (E20 and E200) in the forward scan of CPP and repassivation potentials (ER10, ER1 and ERCO) from the reverse scan. The highest the breakdown potential means the higher the potential that needs to be applied to the alloy to force it to corrode rapidly. Table 2 shows that the highest breakdown potential corresponded to the high nitrate solution 12 m $\text{CaCl}_2 + 6 \text{ m Ca}(\text{NO}_3)_2$ $[\text{Cl}^-]/[\text{NO}_3^-] = 6.67$ at 130°C, confirming the inhibition effect by nitrate in spite of the highest temperature of this electrolyte. The lowest breakdown potentials corresponded to the 5 M CaCl_2 solution at 90°C, showing that the passivity of Alloy 22 was most unstable in this concentrated pure chloride solution.

Once the breakdown had occurred, the repassivation potential indicates how low the potential needs to be applied for the alloy to regain a passivity similar to that before breakdown. The lowest repassivation potential was for the 5 M CaCl_2 solution at 90°C, again suggesting that in this solution it is difficult to repassivate Alloy 22 once the breakdown had occurred. In the solution 6 m NaCl + 0.9 m KNO_3 at 100°C, the breakdown potentials were rather positive but the repassivation potentials were low, that is, the chromium oxide film was initially resistant to breakdown but once localized corrosion was nucleated, the repassivation potentials were rather low (similar to that of 1 M NaCl at 90°C). The solutions at the lower temperature (80°C) and the solution with high nitrate 12 m $\text{CaCl}_2 + 6 \text{ m Ca}(\text{NO}_3)_2$ had the highest repassivation potentials, in spite the latter solution was at 130°C.

Corrosion Mode

Table 1 describes the corrosion characteristics of all the tested specimens after the cyclic potentiodynamic polarization (CPP) tests through optical observation in a stereomicroscope at X20 magnification. Figure 1 shows the corroded specimen after the CPP in 5 M CaCl_2 at 90°C. Figure 1 is a typical mode of attack of Alloy 22 in this solution and it has been observed and described before.⁴⁻⁵ The attack in Figure 1 is termed massive localized corrosion. It is a localized corrosion since it starts at one spot (generally at the crevice former or gasket interface with the metal) and then it propagates over the rest of the specimen following the direction of gravity. Figure 2 shows that the massive attack can also start as corrosion pits on the non-creviced surface of the specimen (short-transverse section of the PCA specimen) and propagating down producing a reverse comet-like feature.

Figures 3 and 4 show the aspect of the specimens polarized in 12 m $\text{CaCl}_2 + 6 \text{ m Ca}(\text{NO}_3)_2$ at 130°C. Even though the temperature was 40°C higher and the specimens were polarized to 900 mV higher than for the specimens polarized in 5 M CaCl_2 at 90°C (Figures 1 and 2), the attack shown in Figures 3 and 4 was more contained than in Figures 1 and 2. This could be the beneficial effect of nitrate in the solution. In the $\text{CaCl}_2 + \text{Ca}(\text{NO}_3)_2$ solution the attack occurred only on the metal surface exposed to the bold solution, away from the crevice formers (Figures 3 and 4). The attack in Figures 3-4 could be associated to a form of pitting corrosion, even though the attack in Alloy 22 is shallow and wide as compared to the typical pitting corrosion observed for example in austenitic stainless steels.⁹

Figure 5 shows the corrosion mode of Alloy 22 after CPP test in 1 M NaCl at 90°C. The appearance of the specimen is typical for this type of environment.¹⁻² There is a yellow and iridescent transpassivity in the boldly exposed surfaces and deep crevice corrosion following the outline of the crevice formers in the occluded areas.⁴⁻⁵ The crevice corrosion attack is bright and crystallographic, showing outlines of grains and even planes inside of the grains.

Figures 6 and 7 show the effect of the temperature on the Alloy 22 susceptibility to crevice corrosion in 6 m NaCl + 0.9 m KNO_3 . At 80°C, the specimen shows mostly iridescent transpassivity in the boldly exposed surfaces and little or no dull crevice corrosion under the crevice formers (Figure 6). At 100°C (Figure 7), the specimen shows a higher amount of dull crevice corrosion and also some spots of crystalline crevice corrosion. The aspect of the crystallographic crevice corrosion is similar to types of attack found in pure chloride solution (for example in 1 M NaCl, Figure 5).



Figure 1. Specimen AY008 after CPP testing in 5 M CaCl_2 at 90°C showing Typical Massive Localized Attack, Magnification $\sim X 8$



Figure 3. Alloy 22 Specimen AY011 after CPP in 12 m CaCl_2 + 6 m $\text{Ca}(\text{NO}_3)_2$ at 130°C Magnification $\sim X 8$



Figure 2. Specimen AY008 after CPP testing in 5 M CaCl_2 at 90°C showing Typical Massive Localized Attack on the ST, Non-Creviced Face

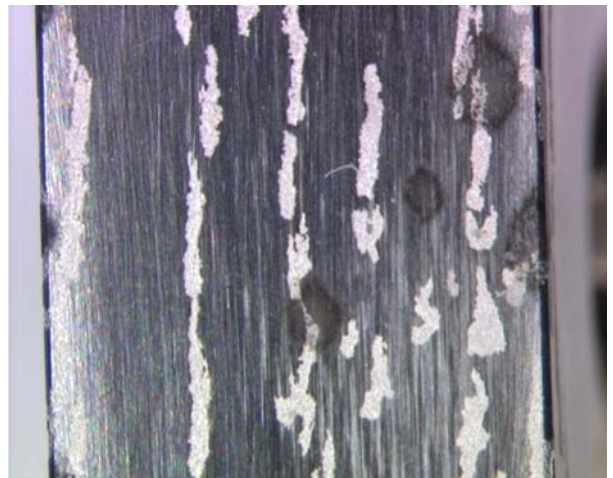


Figure 4. Alloy 22 Specimen AY011 after CPP in 12 m CaCl_2 + 6 m $\text{Ca}(\text{NO}_3)_2$ at 130°C showing Localized Attack on the ST Face (non-creviced), Magnification $\sim X 8$



Figure 5. Alloy 22 Specimen AY009 after CPP in 1 M NaCl at 90°C showing Major Transpassivity in the bold areas. Crevice Corrosion under CF, Magnification ~X 8



Figure 7. Alloy 22 Specimen AY003 after CPP in 6 m NaCl + 0.9 m KNO₃ at 100°C showing Transpassivity in the bold areas and Mostly Dull Crevice Corrosion under CF, Magnification ~X 8

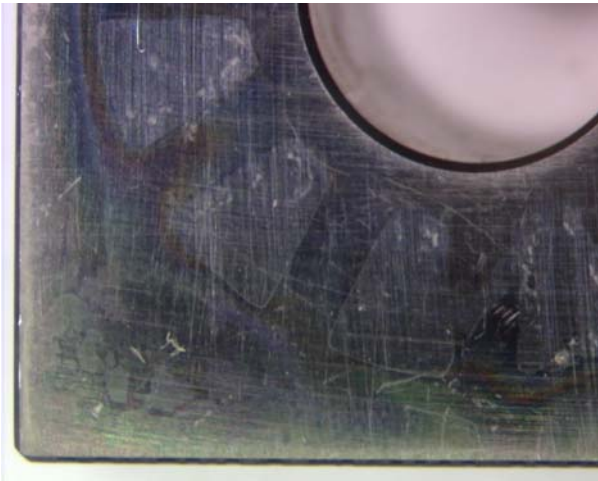


Figure 6. Alloy 22 Specimen AY003 after CPP in 6 m NaCl + 0.9 m KNO₃ at 80°C showing Transpassivity in the bold areas and Little or no Dull Crevice Corrosion under CF, Magnification ~X 8

Comparison with Archive Data

Table 3 shows comparative data between the values of repassivation potential obtained as part of this work (Table 2) and the available data on other type of Alloy 22 specimens in the same environments (salt composition and temperature). Table 3 shows that the results currently presented and the known values of repassivation potential for Alloy 22 are exactly the same. The corollary is that under the tested conditions, the material removed from the mockup behaved exactly the same as the material from laboratory prepared plates. In other words, the values of repassivation potential used to prepare the localized corrosion degradation model for the waste package, also would accurately predict the behavior of a fabricated container.

CONCLUSIONS

- Under the tested conditions, the repassivation potentials (ER1 and ER2) obtained using specimens prepared from a prototype container had the value as the repassivation potentials currently available for specimens fabricated using laboratory welded flat plates
- Values of repassivation potential used in the models to predict the lifetime of the container via localized corrosion accurately represent the conditions of a fabricated container.

ACKNOWLEDGMENTS

This work was partially performed under the auspices of the U. S. Department of Energy by the University of California Lawrence Livermore National Laboratory under contract W-7405-Eng-48. The work was supported by the Yucca Mountain Project, which is part of the DOE Office of Civilian Radioactive Waste Management (OCRWM).

DISCLAIMER

This document was prepared as an account of work sponsored by an agency of the United States Government. Neither the United States Government nor the University of California nor any of their employees, makes any warranty, express or implied, or assumes any legal liability or responsibility for the

accuracy, completeness, or usefulness of any information, apparatus, product, or process disclosed, or represents that its use would not infringe privately owned rights. Reference herein to any specific commercial product, process, or service by trade name, trademark, manufacturer, or otherwise, does not necessarily constitute or imply its endorsement, recommendation, or favoring by the United States Government or the University of California. The views and opinions of authors expressed herein do not necessarily state or reflect those of the United States Government or the University of California, and shall not be used for advertising or product endorsement purposes.

REFERENCES

1. G. M. Gordon, *Corrosion*, 58, 811 (2002)
2. R. B. Rebak and P. Crook, "Influence of the Environment on the General Corrosion Rate of Alloy 22," *PVP-ASME Vol. 483*, pp. 131-136 (American Society of Mechanical Engineers, 2004: New York, NY).
3. ASTM International, Volume 02.04 "Non-Ferrous Metals" Standard B 575 (ASTM International, 2002: West Conshohocken, PA)
4. K. J. Evans, L. L. Wong and R. B. Rebak "Determination of the Crevice Repassivation Potential of Alloy 22 by a Potentiodynamic-Galvanostatic-Potentiostatic Method," *PVP-ASME Vol. 483*, pp. 137-149 (American Society of Mechanical Engineers, 2004: New York, NY).
5. K. J. Evans, A. Yilmaz, S. D. Day, L. L. Wong, J. C. Estill and R. B. Rebak "Comparison of Electrochemical Methods to Determine Crevice Corrosion Repassivation Potential of Alloy 22 in Chloride Solutions," *JOM*, p. 56, January 2005
6. G. O. Ilevbare, K. J. King, S. R. Gordon, H. A. Elayat, G. E. Gdowski and T. S. E. Summers "Effect of Nitrate on the Repassivation Potential of Alloy 22 in Chloride Containing Solutions," Fall 2004 Meeting of the Electrochemical Society, 03-08Oct04, Honolulu, HI (to be published).
7. ASTM International, Volume 03.02, Standards G 5, G 15, G 48, G 59, G 61, G 102 (ASTM International, 2003: West Conshohocken, PA).
8. K. J. King, J. C. Estill, G. A. Hust, M. L. Stuart and R. B. Rebak "Evolution of the Corrosion Potential and Corrosion Rate for Alloy 22 in Chloride plus Nitrate Brines," *CORROSION/2005*, Paper 05607 (NACE International, 2005: Houston, TX)
9. A. J. Sedricks "Corrosion of Stainless Steels" (John Wiley & Sons, Inc., 1996: New York, NY)

Table 1. Specimens, Testing Conditions and Results from CPP

Specimens	Solutions	T (°C)	Observations after CPP
AY001	6 m NaCl + 0.3 m KNO ₃	80	Transpassivity, yellow iridescent, little dull CC
AY002	6 m NaCl + 0.3 m KNO ₃	80	
AY003	6 m NaCl + 0.9 m KNO ₃	80	Transpassivity, yellow iridescent, little dull CC
AY004	6 m NaCl + 0.9 m KNO ₃	80	
AY005	6 m NaCl + 0.9 m KNO ₃	100	Transpassivity and –mostly dull- CC
AY006	6 m NaCl + 0.9 m KNO ₃	100	
AY007	5 M CaCl ₂	90	Massive attack outside CF, IGA on base metal, PC on ST face
AY008	5 M CaCl ₂	90	
AY009	1 M NaCl	90	Transpassivity, yellow, abundant deep CC
AY010	1 M NaCl	90	
AY011	11.4 m CaCl ₂ + 5.4 m Ca(NO ₃) ₂	130	Substantial string-like localized attack outside CF
AY012	11.4 m CaCl ₂ + 5.4 m Ca(NO ₃) ₂	130	
CPP = Cyclic Potentiodynamic Polarization, CC= Crevice Corrosion, CF = Crevice Former, IGA = Intergranular Attack, PC = Pitting Corrosion, ST = Short Transverse			

**Table 2. Corrosion Potential, Corrosion Rate and Parameters from CPP
All Potentials in mV, SSC**

Specimens	E _{corr} 24 h	CR (µm/year)	E20	E200	ER10	ER1	ERCO
AY001	153	0.239, 0.225, 0.192	787	859	761	686	714
AY002	-43	0.430, 0.465, 0.528	786	843	743	430	682
Average	55	0.347	787	851	752	558	698
SD	139	0.144	1	11	13	181	23
AY003	-452	0.362, 0.302, 0.292	738	846	700	582	NA
AY004	-433	0.178, 0.149, 0.147	701	848	684	535	NA
Average	-443	0.238	720	847	692	559	
SD	13	0.092	26	1	11	33	
AY005	-473	0.334, 0.279, 0.324	465	776	554	-52	-75
AY006	-453	0.218, 0.209, 0.226	588	787	597	-34	-74
Average	-463	0.265	527	782	576	-43	-75
SD	14	0.055	87	8	30	13	1
AY007	-384	0.963, 0.870, 0.815	108	138	-52	-93	-73
AY008	-352	0.361, 0.370, 0.300	112	139	-78	-154	-169
Average	-368	0.613	110	139	-65	-124	-121
SD	23	0.3	3	1	18	43	68
AY009	-523	1.917, 1.705, 1.590	441	713	69	-42	-54
AY010	-535	1.718, 1.562, 1.398	486	724	78	-44	-52
Average	-529	1.648	464	719	74	-43	-53
SD	8	0.175	32	8	6	1	1
AY011	108	0.092, 0.096, 0.091	931	1038	798	760	783
AY012	41	0.192, 0.184, 0.181	762	1027	801	781	811
Average	75	0.139	847	1033	800	771	797
SD	47	0.051	120	8	2	15	20

**Table 3. Comparison Between Current and Archive Results
All Potentials in mV, SSC**

Material/ Data Source	ER1	ERCO	ER, CREV
1 M NaCl, 90°C			
Current PCA Mockup (Table 2)	-43 ± 1	-53 ± 1	NA
Archive MA MCA Ref. 4-5	-80 ± 19	-49 ± 16	-30 ± 8
Archive ASW MCA Ref. 4-5	NA	NA	-99 ± 9
5 M CaCl ₂ , 90°C			
Current PCA Mockup (Table 2)	-124 ± 43	-121 ± 68	NA
Archive MA MCA Ref. 5	-182 ± 7	-121 ± 63	NA
Archive ASW MCA Ref. 5	-175 ± 10	-174 ± 15	-130 ± 3
6 m NaCl + 0.9 m KNO ₃ , 100°C			
Current PCA Mockup (Table 2)	-43 ± 13	-75 ± 1	NA
Archive ASW MCA Ref. 6	-49 ± 27	-63 ± 23	NA
MCA = Multiple Crevice Assembly (lollipop), ER,CREV obtained using the Tsujikawa-Hisamatsu Electrochemical (THE) Method (Ref. 4-5)			